Available online at www.sciencedirect.com

ScienceDirect

Transportation Research Procedia 70 (2023) 123–129

Transportation Research Procedia

www.elsevier.com/locate/procedia

8th International Electric Vehicle Conference (EVC 2023)

Maximizing wireless power transmission for electric vehicles with high-intensity laser power beaming and optical orthogonal frequency division multiplexing

Jeongsook Eom[a], Gunzung Kim[a], Yongwan Park[a,*]

[a]*Yeungnam University, 280, Daehak-Ro, Gyeongsan, Gyeongbuk 38541, South Korea*

Abstract

This paper presents a method for determining the optimal power transmission path for wirelessly charging electric vehicles using high-intensity laser power beaming in environments with multiple power transmitters and receivers. The proposed method uses an optical orthogonal frequency division multiplexing system. The power receiver selects the optimal power transmitter and wireless power channel based on the maximum power requirement. The paper also validates the proposed method through simulation and experimentation.

Keywords: wireless power transfer; high-intensity laser power beaming; optical orthogonal frequency division multiple access, multiple transfers and receivers

1. Introduction

Electric vehicles (EVs) have gained momentum in recent years as a solution to the environmental issues caused by internal combustion engines (ICEs) (China M, 2016). Still, the widespread adoption of EVs depends on several factors, including the total cost of ownership and charging time, which significantly impact consumer purchasing decisions (Ashfaq et al., 2021). An EV with a larger battery capacity can run for more longer periods on a single charge, but this also increases the cost and weight of the EV, resulting in lower energy efficiency (El-Bayeh et al, 2021). Additionally, the current method of plug-in charging can be cumbersome, poses safety concerns, and requires a significant amount of charging time; public charging stations may also be susceptible to damage and negatively impact the appearance of

* Corresponding author. Tel.: +82-53-810-3942.
E-mail address: ywpark@yu.ac.kr

10.1016/j.trpro.2023.11.010

cities. To overcome these challenges, wireless power transmission (WPT) is gaining widespread attention as a potential solution, allowing for the miniaturization of batteries, and increasing the maximum range of an EV (Li and Mi, 2014; Baronti et al, 2016; Bi et al, 2016; Shadid et al, 2016; Di et al, 2015). WPT for charging EV is a promising approach with great potential to accelerate EV acceptance through users' higher satisfaction, reducing EV cost, and increasing driving range and capability (Trivino-Cabrera, 2020). A WPT system based on high-intensity laser power beaming (HILPB) provides an optimal solution for wireless charging EVs from several meters (Bhatti et al, 2016; Sprangle et al, 2015). Still, the problem of optimal path configuration for charging EVs remains unexplored (Massa et al, 2013; Ahn and Hong, 2013; Lee and Cho, 2013; Johari et al, 2014; Mou and Sun, 2015). This paper proposes a method to determine the optimal power transmission path in environments where multiple power transmitters (PTXs) and power receivers (PRXs) are operated simultaneously.

2. Structure and operation of wireless power transmission based on high-power laser beam

Zhou and Jin presented a model for a photovoltaic (PV) array operating under the Gaussian laser beam condition (Zhou and Jin, 2016). Their proposed model represents the PV panel as an $m \times n$ network of PV cells arranged in columns and rows. Fig. 1(a) depicts the arrangement of individual PV cells, while Fig. 1(b) shows the calculated normalized irradiance profile model on each numbered PV cell in a 5×5 PV panel (MH GoPower Company, 2016). A previous study proposed a novel approach for wireless power transfer to an EV that had stopped at an intersection using HILPB (Kim et al, 2021). The operational process was confirmed through simulations. This method entails the transmission of a pilot laser signal with a power limit corresponding to MPE Class 1 in all directions where power can be supplied (Laser Institute of America, 2014), along with the location of the PRX requested by the global positioning system (GPS). The PTX estimates the maximum power received from the pilot signal and selects the PTX that provides the highest power supply efficiency. The exact location of the PRX and the PV panel is still being determined due to GPS errors (Zabalegui et al, 2020). The PTX transmits a pilot signal in all directions that the HILPB can transmit to determine the exact center of the PV panel mounted on the PRX since the panel is most efficient when the HILPB is supplied to the center. The PTX identifies the direction that receives the most power by converting the pilot signal into electric power. As the pilot signal can only be transmitted in one direction at a time, the number of directions in which the pilot signal can be transmitted is proportional to the direction in which the PTX transmits the HILPB. As a result, the time to transmit the pilot signal is lengthened, while the time to transmit the HILPB is reduced, which is crucial because the time spent at the intersection is limited. To obtain a significant amount of power, it is necessary to shorten the time required to locate the precise location of the PRX and PV panels.

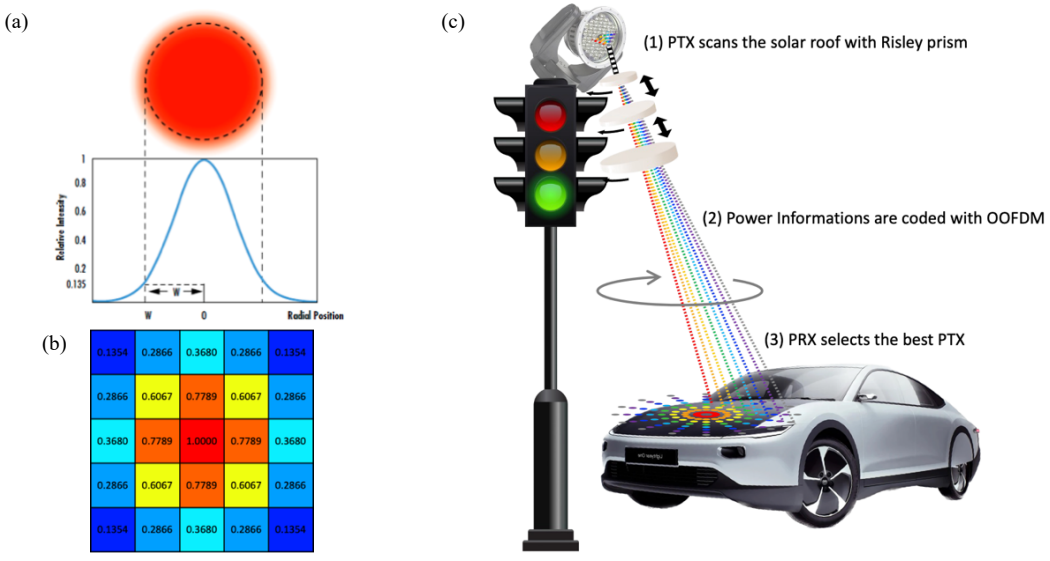

Fig. 1. (a) Gaussian distribution (b) Energy distribution on PV panel (c) Operating concept based on a high-power laser beam and Risley prism.

2.1 System model

We introduce a new method for transmitting pilot signals in multiple directions concurrently using optical orthogonal frequency division multiple access (OOFDMA), wavelength division multiple access (WDMA), and a Risley prism (A, 2018; Azim, 2018; Ghassemlooy et al, 2019; Li et al, 2019; Zhou et al, 2014) represented in Fig 1(c) and 2. Our previous approach to generating the pilot signal uses optical code division multiple access (OCDMA) using a unipolar laser pulse stream (Yang and Kwong, 2002; Kwong and Wang, 2013; Ghafouri-Shiraz and Karbassian, 2012; Kim and Park, 2016; Kim and Park, 2018; Kim and Park, 2018; Kim et al, 2021), which generates seven bits of power information into 49 optical signals. On the other hand, OOFDMA involves more intricate signal processing than unipolar OCDMA but generates 48 bits of power information into only 24 optical signals, enabling more electric power information to be transmitted in less time. WDMA is an optical communication method that uses multiple laser wavelengths simultaneously and can transmit and receive multiple wavelengths of optical signals simultaneously in proportion to the number of wavelengths used. Risley prisms employ the same central axis but differ in their characteristics, refractive index, and rotation speed to create patterns with varying spacing and shapes. Using OOFDMA to generate power transmission information for each wavelength and send it to the prism, the pilot signal can be transmitted in multiple directions simultaneously due to the difference in laser refractive index according to wavelength. Although transmitting more information than traditional methods is required, it is possible to simultaneously transmit pilot signals in more directions in a shorter time by using all three optical technologies.

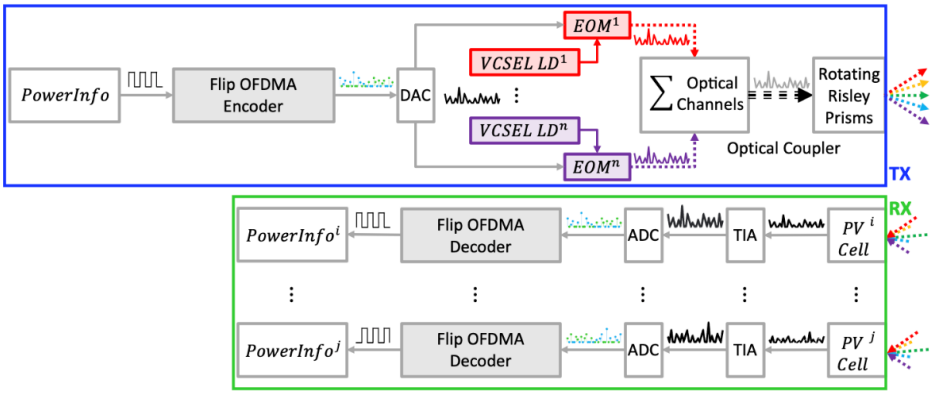

Fig. 2. Overall system model based on an optical orthogonal frequency division multiple access and Risley prism.

As shown in Fig. 3, the pilot signal utilized by the PTX comprises four distinct components: device identification (ID), angle ID, maximum power, and cyclic redundancy check (CRC). The device ID, consisting of 16 bits, serves as a unique identifier for the PTX. The Risley prism, a device utilized for producing scanning patterns, comprises three wedge prisms; one side of the prism is shallower than the other side. The center axis of all three prisms is coaxial, and the three prisms can independently rotate around the center axis, producing distinct scanning patterns. The angle ID, comprising 16 bits, represents the angle to which each prism is rotated about its center axis in a Risley prism. The maximum power, expressed in watts and using 8 bits, denotes the maximum power of the continuous wave (CW) laser that the PTX can transmit. Additionally, the CRC, consisting of 8 bits of checksum data, is generated by performing CRC-8 on the 40 bits corresponding to the device ID, angle ID, and maximum power. To ensure the data transmission process is error-free, the PRX, a device utilized for receiving data, generates a checksum using CRC-8 for the 40 bits received and compares it with the 8 bits of CRC received.

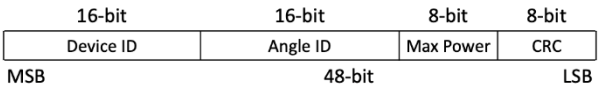

Fig. 3. Frame structure of the pilot signal.

It is recommended that the spacing between the Risley prisms utilized in transmitting data should be adjusted based on the distance between the PTX and PRX, as well as the size of the PV panel. When the distance between the PTX and PRX is close or when the PV panel is large, the prisms should be spaced closer together to increase the size of the pattern. Conversely, when the PTX to PRX distance is longer, or the PV panel is small, the prisms should be spaced farther apart to reduce the size of the pattern. The pilot signal, PowerInfo, is encoded using the Flip OFDMA technique to convert it into a signal that can be transmitted represented by Fig 4(a). The analog signal generated by the digital-to-analog converter (DAC) is used to produce an analog laser utilizing an external optical modulator (EOM) and a laser diode (LD).

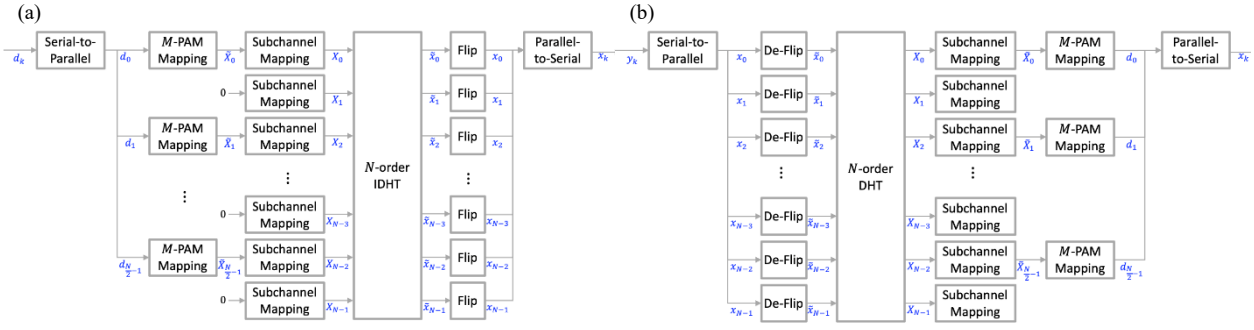

Fig. 4. (a) Flip-OFDM encoder of the pilot signal transmitter (b) Flip-OFDM decoder of the pilot signal receiver.

Additionally, the analog laser signal generated by performing the same operation at multiple laser wavelengths simultaneously is combined into a single signal via an optical coupler. The laser signal transmitted to the Risley prism undergoes refraction by the wavelength each time it passes through the prism before being transmitted. Following the transmission of the laser signal, the Risley prism is rotated by a predetermined angle. The PRX, on the other hand, utilizes a PV panel to convert the received laser signal into an analog signal utilizing a transimpedance amplifier (TIA) and a digital signal utilizing an analog-to-digital converter (ADC). Subsequently, decoding is performed utilizing the Flip OFDMA technique to generate PowerInfo represented by Fig 4(b). After receiving all PowerInfo sent by other PTXs, count the number of receptions by device ID and select the PTX with the highest number of device IDs. The ratio of the number of device IDs received by the PRX to the number of device IDs transmitted by the PTX indicates the reception rate of the HILPB transmitted to the PV panel. The greater the number of identical Device IDs and Angle IDs, the higher the HILPB received by the PV panel. The angle ID indicates whether the prism center axis matches the center axis of the PV panel. Moving the prism's center axis in a direction with many identical angle IDs makes it more likely that the two center axes will match. Using Max Power and Reception Rate, you can estimate the maximum power that can be received. If the amount of light received does not exceed the PV panel's limit, all HILPB can be used for power conversion. However, if the power received from a single PTX is insufficient, multiple PTXs can be selected to provide power as required.

2.2 Operating sequence

As shown in Fig. 5, the proposed method for supplying power to EVs at intersections via vehicle-to-infrastructure (V2I) communication involves several steps. Firstly, when an EV arrives at an intersection, it stops and broadcasts a power demand signal to its neighboring power transmitting devices, which are PTXs installed at the intersection, using V2I communication. This power demand signal contains the location information and size of the PV panel of the EV. Upon receiving the power demand signal via V2I, the PTX generates PowerInfo, which includes device ID, angle ID, max power, and CRC information. The device ID is a unique number that identifies the power-transmitting device, while the angle ID indicates the rotation angle relative to the prism's center. The max power specifies the maximum power that can be transmitted, and the CRC information validates the received PowerInfo. The PTX then adjusts the distance between the prisms according to the location of the PRX and the size of the PV panel so that the PV panel

receives all lasers refracted through the prisms. After the PTX sends the PowerInfo to the EV, the Risley prism is rotated by a predetermined angle. The PRX then interprets the PowerInfo received by the PV panel, determines the wavelength-specific position of the laser relative to the center of the PV panel, and estimates the maximum power it can receive based on this information. The PRX selects a PTX to provide the required power based on the power received and predicted over time. Since the HILPB can receive power from more than one PTX, in case one PTX does not provide enough power, multiple PTXs can be selected simultaneously to provide power.

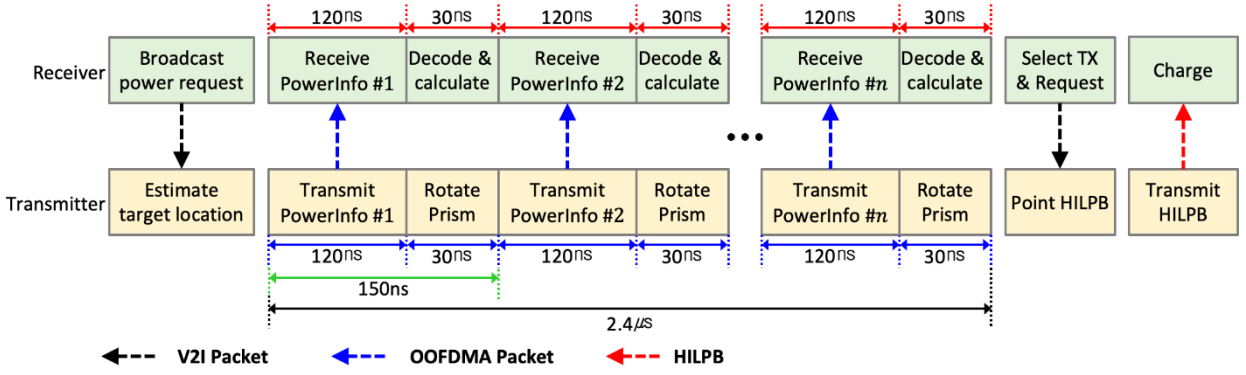

Fig. 5. Basic handshaking protocol between PTX and PRX.

3. Operation example

When an EV approaches the intersection and waits to signal, the EV-mounted RX broadcasts its location and the position of its PV panel through V2I and requests power. At the intersection, four traffic lights are located at each corner, and each traffic light is equipped with a PTX powered by a HILPB represented in Fig 6. To provide power to the EV, the four PTXs adjust their prisms based on the distance and size of the PV panel on the EV and send pilot signals for every angle at which power can be transmitted. For T1, the center axis of the Risley prism was received at the corner of the PV panel, and as a result, some of the pilot signals were received by the PV panel.

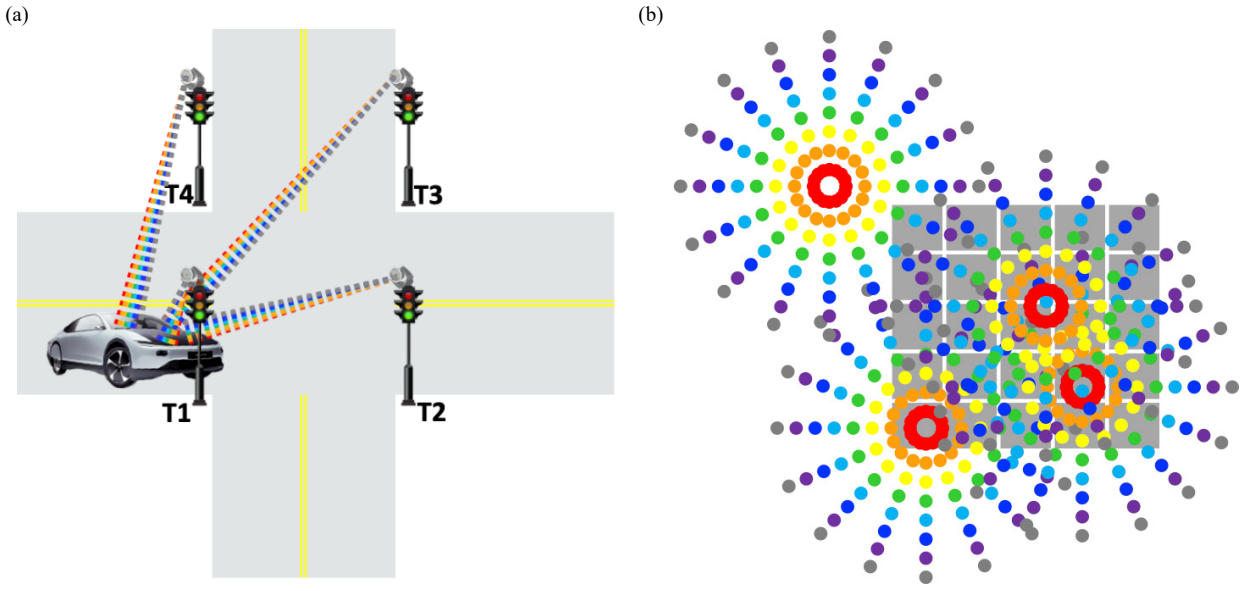

Fig. 6. (a) PTXs send their PowerInfo to a PRX (b) Four patterns of PowerInfo have arrived at the PV panel of the EV.

As different PTXs have different patterns and numbers of pilot signals received by the PV panel due to GPS and aiming errors, the pilot signal from T3 was found to be received by the PV panel the most, followed by the pilot signal from T2 represented in Fig 7. On the other hand, the center axis of the Risley prism for T4 was offset from the PV panel, leading to the least number of pilot signals being received by the PV panel. The EV selects the PTX with the most pilot signals to request power transmission, and the selected PTX transmits a HILPB to the center axis point of the prism used to transmit the pilot signal. The EV utilizes a PV panel to convert the received HILPB into electricity, which is then used to charge the battery. When the battery is fully charged or the signal changes, the EV notifies of the power interruption through V2I. The PTX stops transmitting power, and the EV proceeds toward.

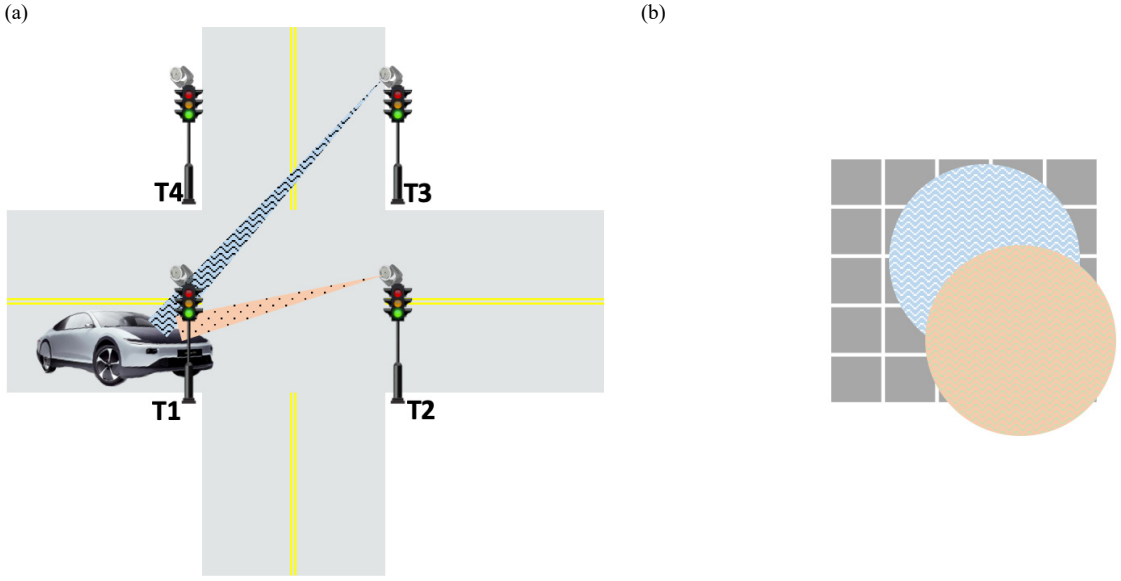

Fig. 7. (a) PTX T2 and T3 are selected for electric power transmission (b) HILPB from T2 and T3 have arrived at the PV panel of the EV

4. Conclusion

Our study proposes a novel WPT system utilizing HILPB technology to decrease the size of EV batteries and extend their driving range. This system incorporates OOFDMA and Risley prism to precisely position the receiver and enabling power delivery from multiple sources. We have developed a WPT system and pairing algorithm, which have been validated through simple simulation. In our proposed a method, it is possible to reduce the waiting time at traffic lights by enabling a PTX to continue transmitting power to another PRX while waiting at a red traffic light after completing an electric power transfer to the first PRX. The proposed system and algorithm provide a promising solution for efficient and reliable WPT in EVs, which could significantly improve their performance and contribute to the widespread adoption of EVs.

Acknowledgments

This research was supported by Basic Science Research Program through the National Research Foundation of Korea (NRF) funded by the Ministry of Education (NRF-2021R1A2B5B02086773, NRF-2021R1A6A1A03039493, NRF-2022R1I1A1A01070998).

References

A. Li, 2018. Double-Prism Multi-Mode Scanning: Principles and Technology. Springer.

Ahn, D., Hong, S., 2013. Effect Of Coupling Between Multiple Transmitters or Multiple Receivers on Wireless Power Transfer. IEEE Transactions on Industrial Electronics 60.7, 2602–2613.

Ashfaq, M., Butt, O., Selvaraj, J., Rahim, N., 2021. Assessment of Electric Vehicle Charging Infrastructure and Its Impact on The Electric Grid: A Review. International Journal of Green Energy 18, 1–30.

Azim, A. W., 2018. Signal Processing Techniques for Optical Wireless Communication Systems. Ph.D. Dissertation, Universite Grenoble Alpes.

Baronti, F., Chow, M. Y., Ma, C., Rahimi-Eichi, H., Saletti, R., 2016. E-Transportation: The Role of Embedded Systems in Electric Energy Transfer from Grid to Vehicle. EURASIP Journal on Embedded Systems 2016. 1-12.

Bhatti, A. R., Salam, Z., Aziz, M. J. B. A., Yee, K. P., 2016. A Critical Review of Electric Vehicle Charging Using Solar Photovoltaic. International Journal of Energy Research 40.4, 439–461.

Bi, Z., Kan, T., Mi, C. C., Zhang, Y., Zhao, Z., Keoleian, G. A., 2016. A Review of Wireless Power Transfer for Electric Vehicles: Prospects to Enhance Sustainable Mobility. Applied Energy 179, 413-425.

China, M., China Vehicle Environmental Management Annual Report 2016. Ministry Of Ecology and Environment of The People's Republic of China: Beijing, China, 2016.

Di Capua, G., Sánchez, J. A., Cabrera, A. T., Cabrera, D. F., Femia, N., Petrone, G., Spagnuolo, G., 2015. A Losses-Based Analysis for Electric Vehicle Wireless Chargers. In Proceedings of the 2015 International Conference on Synthesis, Modeling, Analysis and Simulation Methods and Applications to Circuit Design, Turkey, 1–4.

El-Bayeh, C. Z., Alzaareer, K., Aldaoudeyeh, A. M. I., Brahmi, B., Zellagui, M., 2021. Charging and Discharging Strategies of Electric Vehicles: A Survey. World Electric Vehicle Journal 12.1, 11.

Ghafouri-Shiraz, H., Karbassian, M. M., 2012. Optical CDMA Networks: Principles, Analysis and Applications. John Wiley & Sons.

Ghassemlooy, Z., Popoola, W., Rajbhandari, S., 2019, Optical Wireless Communications: System and Channel Modelling with MATLAB. CRC Press.

Johari, R., Krogmeier, J. V., Love, D. J., 2014. Analysis and Practical Considerations in Implementing Multiple Transmitters for Wireless Power Transfer via Coupled Magnetic Resonance. IEEE Transactions on Industrial Electronics 61.4, 1774–1783.

Kim, G., Ashraf, I., Eom, J., Park, Y., 2021. Optimal Path Configuration with Coded Laser Pilots for Charging Electric Vehicles using High Intensity Laser Power Beams. Applied Sciences 11.9, 3826.

Kim, G., Park, Y., 2016. Lidar Pulse Coding for High Resolution Range Imaging at Improved Refresh Rate. Optics Express 24.21, 23810–23828.

Kim, G., Park, Y., 2018. Independent Biaxial Scanning Light Detection and Ranging System Based on Coded Laser Pulses without Idle Listening Time. Sensors 18.9, 2943.

Kim, G., Park, Y., 2018. Suitable Combination of Direct Intensity Modulation and Spreading Sequence for Lidar with Pulse Coding. Sensors 18.12, 4201.

Kwong, W. C., Yang, G. C., 2013. Optical Coding Theory with Prime. CRC Press.

Laser Institute of America, 2014. Ansi Z136.1–2014: American National Standard for Safe Use of Lasers; Laser Institute of America, 2014.

Lee, K., Cho, D. H., 2013. Diversity Analysis of Multiple Transmitters in Wireless Power Transfer System. IEEE Transactions on Magnetics 49.6, 2946-2952.

Li, S., Mi, C. C., 2014. Wireless Power Transfer for Electric Vehicle Applications. IEEE Journal of Emerging and Selected Topics in Power Electronics 3.1, 4–17.

Li, S., Cao, J., Cheng, Y., Meng, L., Xia, W., Hao, Q., Fang, Y., 2019. Spatially Adaptive Retina-Like Sampling Method for Imaging Lidar. IEEE Photonics Journal 11.3, 1–16.

Massa, A., Oliveri, G., Viani, F., Rocca, P., 2013. Array Designs for Long–Distance Wireless Power Transmission: State–of–the–Art and Innovative Solutions. Proceedings of the IEEE 101, 1464–1481.

MH GoPower Company. 2016. MH VMJ PV Cell–Array Datasheet, Taiwan.

Mou, X., Sun, H., 2015. Wireless Power Transfer: Survey and Roadmap. In Proceedings of the 2015 IEEE 81st Vehicular Technology Conference, 1–5.

Shadid, R., Noghanian, S., Nejadpak, A., 2016. A Literature Survey of Wireless Power Transfer. In Proceedings of the 2016 IEEE International Conference on Electro Information Technology, USA, 0782–0787.

Sprangle, P., Hafizi, B., Ting, A., Fischer, R., 2015. High–Power Lasers for Directed–Energy Applications. Applied Optics 54.31, F201–F209.

Trivino-Cabrera, A., González-González, J. M., Aguado, J. A., 2020. Wireless Power Transfer for Electric Vehicles: Foundations and Design Approach. Springer.

Yang, G. C., Kwong, W. C., 2002. Prime Codes with Applications to CDMA Optical and Wireless Networks. Artech House.

Zabalegui, P., De Miguel, G., Perez, A., Mendizabal, J., Goya, J., Adin, I., 2020. A Review of The Evolution of The Integrity Methods Applied in GNSS. IEEE Access 8, 45813-45824.

Zhou, J., Qiao, Y., Cai, Z., Ji, Y., 2014. An Improved Scheme for Flip-OFDM Based on Hartley Transform in Short-Range IM/DD Systems. Optics Express 22.17, 20748–20756.

Zhou, W., Jin, K., 2016. Optimal Photovoltaic Array Configuration Under Gaussian Laser Beam Condition for Wireless Power Transmission. IEEE Transactions on Power Electronics 32.5, 3662-3672.